Research papers

Phytoplankton productivity in a turbid buoyant coastal plume

Oscar Schofield [a], Mark Moline [b], Brownyn Cahill [a], Thomas Frazer [c], Alex Kahl [a], Matthew Oliver [b], John Reinfelder [d], Scott Glenn [a], Robert Chant [a,*]

[a] Coastal Ocean Observation Lab, Institute of Marine and Coastal Sciences, School of Environment and Biological Sciences, Rutgers University, New Brunswick, NJ 08901, USA
[b] Marine Sciences Department, University of Delaware, Lewes, DE 19958, USA
[c] University of Florida, Institute of Food and Agricultural Science, Department of Fisheries and Aquatic Sciences, 7922 NW 71st Street, Gainesville, FL 32653, USA
[d] Department of Environmental Sciences, School of Environment and Biological Sciences, Rutgers University, New Brunswick, NJ 08903-0231, USA

ARTICLE INFO

ABSTRACT

The complex dynamics associated with coastal buoyant plumes make it difficult to document the interactions between light availability, phytoplankton carbon fixation, and biomass accumulation. Using real-time data, provided by satellites and high frequency radar, we adaptively sampled a low salinity parcel of water that was exported from the Hudson river estuary in April 2005. The water was characterized by high nutrients and high chlorophyll concentrations. The majority of the low salinity water was re-circulated within a nearshore surface feature for 5 days during which nitrate concentrations dropped 7-fold, the maximum quantum yield for photosynthesis dropped 10-fold, and primary productivity rates decreased 5-fold. Associated with the decline in nitrate was an increase in phytoplankton biomass. The phytoplankton combined with the Colored Dissolved Organic Matter (CDOM) and non-algal particles attenuated the light so the 1% light level ranged between 3 and 10 m depending on the age of the plume water. As the plume was 10–15 m thick, the majority of the phytoplankton were light-limited. Vertical mixing within the plume was high as indicated by the dispersion of injected of rhodamine dye. The mixing within the buoyant plume was more rapid than phytoplankton photoacclimation processes. Mixing rates within the plume was the critical factor determining overall productivity rates within the turbid plume.

© 2013 Elsevier Ltd. All rights reserved.

1. Introduction

Buoyant coastal currents are a global feature delivering nutrients, sediments, and in urbanized watersheds, pollutants to coastal waters. Along the Eastern seaboard of the United States there are numerous estuarine plumes fed by rivers that typically have maximum discharge rates on the order of 1000 m^3 s^{-1}. In the Mid-Atlantic Bight (MAB), the Hudson River is a prominent feature which has moderate flow (~1000 m^3 s^{-1}) but is a major source of nutrients and chemical contaminants (Adams et al., 1998). The anthropogenic "potency" reflects the river's century of urbanization, which has resulted in high concentrations of contaminants. For example the Hudson River has higher than average concentrations for 58 of the 59 chemicals monitored by the United States Environmental Protection Agency (Adams et al., 1998). Additionally, the Hudson River has close to 100 m^3 s^{-1} of treated sewage flow into the lower estuary and 90% of the associated inorganic nitrogen is exported unassimilated to the coastal ocean. The fate of these compounds is related to the transport and transformation

processes occurring within the Hudson River and in the adjacent coastal ocean (Moline et al., 2008).

The transport of nutrients and pollutants within the Hudson River outflow depends on the structure and coherence of the buoyant plume once it enters the MAB. The shape and lifetime of buoyant plumes is controlled by local bottom topography, ocean circulation, tides, and wind (Garvine, 1999; Chapman and Lentz, 1994, Yankovsky and Chapman, 1997; Munchow and Garvine, 1993; Fong and Geyer, 2001). The Hudson River buoyant plume often forms a re-circulating entrapped Hudson River water parcel at the mouth of the estuary (Chant et al., 2007). This has the potential to trap material near the estuarine outflow where it can potentially operate as a naturally occurring batch culture for the phytoplankton (Moline et al., 2008). This allows for biogeochemical transformations of the particulate and dissolved organic matter prior to its dispersion across the shelf by winds and ambient shelf circulation. The subsequent shelf-wide dispersion of fresh water from the Hudson is a significant hydrographic feature on the MAB for weeks after leaving the local discharge area (Johnson et al., 2003, Castaleo et al., 2008).

The long lifetime of the buoyant plume has significant implications for the biology and chemistry within the plume. It allows sufficient time for phytoplankton to grow utilizing the ample nutrients provided by the river water (NO$_3^-$ = 15 μM, NH$_4^+$ = 20 μM,

* Corresponding author. Tel.: +1 732 932 6555; fax: +1 732 932 8578.
E-mail address: chant@marine.rutgers.edu (R. Chant).

Fan, 2002). This results in high productivity rates in the buoyant plume that are often 3x higher than in the lower Hudson River (Malone et al., 1996), which is impressive given high phytoplankton productivity rates in the estuary (Howarth et al., 2006). These high productivity rates have the potential to draw down the nutrients and contaminants being discharged. After entering the base of the food chain, these compounds can bio-accumulate and be removed from surface waters via sinking particles (Moline et al., 2008). Given the high concentrations of metals [iron (Fe), copper (Cu) and zinc (Zn), nickel (Ni), cadmium (Cd), lead (Pb), silver (Ag), and mercury (Hg)] present within the Hudson river (Sanudo-Wilhelmy and Gill, 1999, Moline et al., 2008) and the potential for their accumulation in phytoplankton, understanding the factors regulating primary productivity in the buoyant plume is critical.

The initial productivity of the Hudson River plume is not limited by nutrients but rather by the availability of light because the highly turbid waters result in a shallow euphotic zone (Malone et al., 1996, Malone and Chervin, 1979). The turbidity is caused both by suspended sediment from the estuary and by the high phytoplankton productivity in the plume. Stratification within the plume can trap biomass in distinct layers where light levels can vary by orders of magnitude in just a meter. In a well-mixed plume, turbulence is uninhibited by stratification and phytoplankton cells are vertically homogeneous throughout the low saline water and are subject to a vertically averaged light level. This should increase overall light-limitation of cells as at any given time as only a small proportion of the plume is within the euphotic zone. This has significant implications for regulating the acclimation and overall productivity of the phytoplankton (Falkowski and Raven, 2007).

The relative importance of mixing on light availability within buoyant plume of the Hudson River is difficult to assess due to complex spatial dynamics making it difficult to sample using traditional sampling strategies. This is problematic as this is central to understanding the potential synthesis of organic carbon and accumulation of chemical compounds in coastal food webs. In this manuscript, we focus on the optics and mixing within the plume and assess the regulation of phytoplankton production in the re-circulating parcel of low salinity water.

2. Material and methods

As part of the LAgrangian Transport and Transformation Experiment (LATTE) a multi-ship operation was conducted during April 9th to April 22nd 2005 offshore the New York/New Jersey estuary (Fig. 1). For this paper we focus on data collected during a rhodamine dye injection (Houghton et al., 2009) on April 11th. For this manuscript we focus on the river plume's impact on coastal biogeochemistry during the 7 days following that dye injection. This was motivated by past studies that have documented recurrent regions of bottom water hypoxia along southern New Jersey that are related to summer time upwelling (Glenn et al., 2004). This upwelling induced hypoxia hypothesis could never explain the northernmost recurrent low dissolved oxygen zone near the mouth of the Hudson river outflow, prompting the hypothesis that heavy organic matter loading from the river drove the low dissolved oxygen in this zone.

The field effort in 2005 was preceded by a significant Hudson outflow, corresponding to a 10-year flood, associated with the spring thaw of snow and a series of precipitation events. Ships, requisitioned specifically for this experiment, sampled the plume adaptively by using real time data collected by the Coastal Ocean Observation Laboratory (Schofield et al., 2010). The adaptive sampling was enabled by a ship to shore wireless communication grid that allowed data to be transmitted to scientists onboard the ship (Schofield et al., 2002, Glenn and Schofield, 2003, Schofield et al., 2007). The real-time data was provided by the international constellation of ocean sensing satellites, a network of surface current mapping high frequency radar systems, and an autonomous underwater Webb glider. These tools provided spatial maps of the plume over time, which was used to redirect the ship sampling. The communication network allowed the two ships to share data. Taken together, this allowed scientists to conduct sampling of the dynamic river plume throughout the field effort.

During the ship surveys the R/V Cape Hatteras conducted underway physical, biological and chemical sampling with two towed undulating platforms behind the ship that provided vertical profiles at a horizontal resolution nominally at 500 m. One system provided measurements of temperature, salinity, currents, chlorophyll fluorescence and rhodamine dye fluorescence. A second system provided underway chemical sampling with water that was pumped to a LaChat autoanalyzer outfitted to provide continuous surface measurements of nitrate, ammonia, phosphorus and silicate. The autoanalyzer was calibrated throughout the cruise. The second ship, the R/V Oceanus, was used for optical profiling and collection of discrete water samples for phytoplankton pigmentation and ^{14}C productivity measurements (see below).

These shipboard efforts were organized around surface dye experiments used to map the transport and dispersion of the river water. Dye experiments consisted of an injection of rhodamine dye near surface of the Hudson River's outflow as described in Chant et al. (2008). The dye injections were conducted in a parcel of fluid
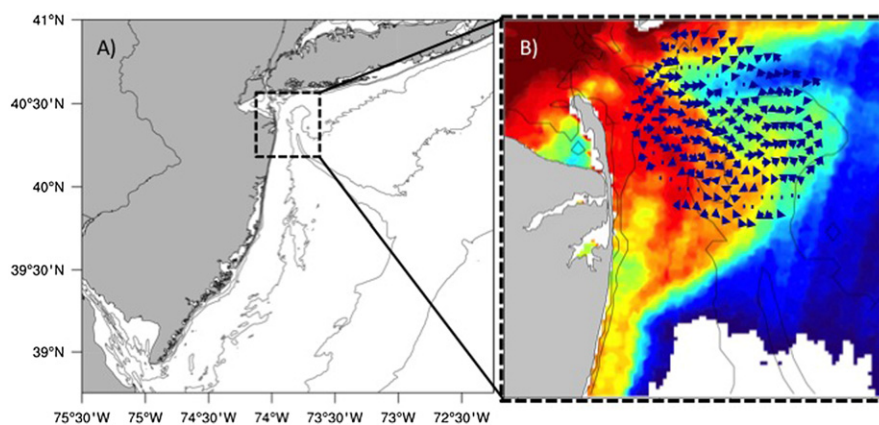

Fig. 1. (A) Maps of the bathymetry for this study area (dotted line box) denotes the general operation area for the LATTE 2005 field experiments offshore the coast New Jersey. (B) An ocean color image during the April 2005 dye injection experiment by the Indian OCM ocean color satellite. Overlaid are the surface currents measured by HF radar that provided continuous updates of surface currents to allow the research vessels to optimize their sampling of the dynamic plume.

during the ebb shortly after it left the estuary. The timing and locations of the dye injections were guided by real-time HF radar data (see below). The dye was tracked using *in situ* flourometers aboard the ships. The dispersion of the dye provided information on overall mixing rates in the low salinity plume.

Remote sensing data. All available satellite data was collected using L-Band and X-band satellite data acquisition systems. The L-Band system was used to track the National Oceanic and Atmospheric Administration (NOAA) Polar Orbiting Environmental Satellites. Products included sea surface temperature (SST) and broad spectrum visible imagery. The X-Band system tracked the United States MODIS (both Terra and Aqua) and India's OCM OceanSat satellites. The resolution of the imagery varied with satellite system, with the Indian OCM system having the highest spatial resolution of 300 m. Significant correlations between the measured chlorophyll *a* and satellite derived estimates were observed for the Mid-Atlantic Bight however satellite-derived chlorophyll were underestimated in the plume (data not shown). Regardless, the ocean color imagery was the most useful satellite data set in assisting the adaptive sampling of the plume as the sea surface temperatures in the river and coastal ocean were similar.

The satellite imagery was complemented with a fully nested array of surface current mapping radars (Kohut and Glenn, 2003, Kohut et al., 2004). Hourly surface currents were measured with an array of CODAR HF Radar systems consisting of 6 long-range (5 MHz) and 2 high-resolution (25 MHz) backscatter systems. For all systems, the beam patterns were calibrated and used in surface current estimates (Kohut and Glenn, 2003). Each site measures the radial components of the ocean surface velocity directed toward or away from the site (Crombie, 1955; Barrick, 1972; Barrick et al., 1977) and the estimated velocity components allow surface currents (upper meter of the water column) to be estimated (Stewart and Joy, 1974).

At each ship station occupied by the RV Oceanus, profiles of temperature ($^\circ$C), salinity, chlorophyll *a* fluorescence (converted to μg L^{-1} using factory calibration coefficients) and dissolved oxygen (mL L^{-1}) were collected with a Seabird SBE CTD, Wetlabs WetStar fluorometer and a SBE oxygen sensor. It should be noted for this study we did not omit day light surface measurements of chlorophyll fluorescence, even though they are likely impacted by fluorescence quenching processes. This was because we used the fluorometric data to choose discrete water depths for phytoplankton pigmentation measurements (see below). Only measured chlorophyll (see below) was used to normalize discrete ^{14}C-incubation data.

Each profile was complemented with a second profile collected with a cage outfitted with Wetlabs Inc. absorption-attenuation meter (ac-9) and 2 Wetlabs Inc. ECO-VSF systems. The ac-9 instrument measured absorption at nine standard wavelengths (412, 440, 488, 510, 555, 630, 650, 676, 715 nm). The ECO-VSF wavelengths were 440, 470, 495, 650, and 880 nm. The optical windows and flow cells were cleaned prior to each deployment. At each station, the instrument was lowered to depth and the instrument was allowed to equilibrate to ambient temperature before data were collected. Data were averaged into 0.25-m depth bins for all subsequent analyses. The instruments were factory calibrated prior to the field season and manufacturer recommended protocols were used to track instrument calibration. Salinity and temperature corrections based on CTD data were applied (Pegau et al., 2001). Whenever possible, daily clean water calibrations were conducted; however, sampling schedules did not always allow for a daily calibration. The drift during the study was negligible ($<$5%) and the precision of the ac-9 data was ± 0.07 m^{-1}.

In situ light fields were calculated for the entire field effort. Shipboard measurements of the downwelling radiation were measured above the sea surface with a Eppley Precision Spectral Pyranometer where the light flux was corrected to provide estimates of photosynthetically available radiation (PAR, integrated light from 400 to 700 nm) assuming a standard solar spectrum (Morel and Smith 1974). The spectral diffuse attenuation coefficient was calculated using the measured spectral inherent optical properties and Hydrolight 4.3 (Mobley 1994). For the Hydrolight runs both the ac-9 and Eco-VSF data were used to initialize the model. The spectral diffuse attenuation coefficients were combined with the surface flux of light to provide the *in situ* light field for any depth or time at a station.

Binned (0.25 m) absorption data collected with the ac-9 were inverted using the optical signature inversion (OSI) model (Schofield et al., 2004), which estimates the optical concentration of phytoplankton, colored dissolved organic matter (CDOM), and non-algal particles. This is based on inverting the bulk ac-9 absorption from a series of idealized absorption curves that represent the major absorbing components in the water column. Phytoplankton absorption represents the average absorption spectra for high and low light adapted cells for the three major spectral classes of phytoplankton (chlorophyll *a–c*, chlorophyll *a–b* and phycobilin containing phytoplankton) (Johnsen et al., 1994). The CDOM and non-algal particles were treated as a series of exponential curves (Kalle, 1966; Bricaud et al., 1981; Green and Blough, 1994) where both the optical weight and slopes were allowed to vary; however the slopes did not vary much in this data set compared to past studies (Schofield et al., 2004; Oliver et al., 2004; Schofield et al., 2006). By varying the magnitude of the optical weights as well as the CDOM and non-algal particle slopes the difference between modeled and ac-9 measured total absorption spectrum was minimized as a function of wavelength. This method also includes some constraints, which have been shown to increase the model accuracy (Oliver et al., 2004; Schofield et al., 2004; Schofield et al., 2006). The stability of the OSI results have been tested by introducing random noise into the ac-9 spectra (± 0.005 m^{-1}across all wavelengths) and there was no spectral bias with a quantitative impact of $<$4% (Schofield et al., 2004).

Water samples from target depths were collected with 10-L Niskin bottles. Phytoplankton assemblages were assessed microscopically and with High Performance Liquid Chromatography (HPLC). Phytoplankton pigments were determined using the method of Van Heukelem and Thomas (2001) to separate and quantify chlorophylls, phaeopigments and carotenoids. Sample aliquots were filtered onto three different filter sizes (0.2, 2.0 and 20 μm). The polycarbonate filters were Osmonics Poretics. After filtration the samples were quick frozen and stored at $-80\ ^\circ$C prior to analysis. They were extracted in 90% acetone (24 h) and sonicated to enhance extraction efficiencies. Pigment peaks were detected with a photodiode array absorption detector (190–800 nm). Pigment standards were purchased from DHI Water and Environment Institute (Denmark) and Sigma-Aldrich Inc. The concentrations were determined with published extinction coefficients (Latasa et al., 1996; Jeffrey et al., 1997). These HPLC values were combined with the discrete radioisotope measurements (below) to provide chlorophyll-normalized measurements.

Phytoplankton carbon fixation rates were measured using two different methods. Bulk size fractionated phytoplankton productivity rates were measured onboard the ship using C^{14} radioisotope techniques. Seawater aliquots were distributed into 2.8 L glass Fernbachs and incubated for 24 h in a temperature controlled environmental van configured to simulate ambient field conditions. The temperature was adjusted before each set of measurements. Fernbachs were illuminated (14 h:12 h light:dark cycle) with cool white fluorescent lights mounted 10 cm above the top of the fernbachs. The mean incident light level at each fernbach was 50 μmol m^{-2} s^{-1}. This value was initially chosen based on optical data in the Hudson River plume collected the year prior during a pilot cruise. Water for these incubations were collected 1–2 below the surface, which was above the 1% light level in the turbid river

and was close to an incident irradiance of 50 µmol m^{-2} s^{-1} on a sunny day. Fernbachs were gently swirled every 6 h to promote resuspension of settled cells although ship motion was generally sufficient for this purpose. At the end of the incubation period, samples were serially filtered through a 20, 2, and 0.2 µm (45 mm diameter) Nucleopore filters. Filters were submerged with EcoScint Fluor and isotope uptake was measured using a manually loaded HiDex Inc. Triathler single vial scintillation counter.

The second radio-isotope method assessed the phytoplankton productivity and photophysiology. Each day, we collected a vertical profile of up to 5 photosynthesis-irradiance curves for different depths. These measurements were made using a temperature-controlled photosynthetron (Prézelin et al., 1992) that allowed 25 one ml aliquots to be incubated simultaneously over a range of light intensities. The vials were incubated for 1 h, filtered onto 0.2 nucleopore filters, submerged into EcoScint Fluor, and also counted on the HiDex Inc. Triathler single vial scintillation counter. A large filtration rig allowed the full curve to be processed with 5–10 min in a darkened radiation van. The resulting data allowed a photosynthesis-irradiance (P–E) curve to be constructed. From the P–E curve the maximum photosynthetic rate (P_{max}, mg C m^{-3} h^{-1}), the light-limited slope (α, mg C m^{-3} h^{-1} (µmol photons m^{-2} s^{-1})$^{-1}$) and the irradiance at which photosynthesis becomes light saturated (E_k, µmol photons m^{-2} s^{-1}) were calculated. These parameters were used to describe the photo-acclimation state of the phytoplankton and when combined with the phytoplankton absorption allowed the quantum yields of carbon fixation to be calculated which is the most sensitive proxy for the assessing the physiological state of the phytoplankton (Bidigare et al., 1989, Cleveland et al., 1989, Smith et al., 1989, Prézelin et al., 1991). Quantum yields were only calculated for the P–E curves. The maximum quantum yield (ϕ_{max}, mol C fixed mol^{-1} photons absorbed) was calculated according to,

$$\Phi_{max} = \alpha / \overline{a}_{ph} \qquad (1)$$

where PAR is the photosynthetically available radiation and $\overline{a}_{ph}$ (m^{-1}) is the spectrally weighted phytoplankton absorption spectra. Values of $\overline{a}_{ph}$ were calculated according to Eq. (2).

$$\overline{a}_{ph} = \int_{400\ nm}^{700\ nm} Ed(\lambda) \times a_{ph}(\lambda) d\lambda / \int_{400\ nm}^{700\ nm} Ed(\lambda) d\lambda \qquad (2)$$

Calculating spectrally weighted absorption was critical in these waters given the skewed light field found in and below the turbid river plume (Fig. 2). The absorption spectra were provided by the ac-9 OSI method (described above). Given that α in the P–E curve is wavelength dependent (Tanada, 1951, Schofield et al., 1990), it was also corrected for the spectrally skewed light field using the methods outlined in Arrigo and Sullivan (1992). In brief this method calculates the mismatch between the absorbed radiation in the photosynthethron (based on the spectrum of light within the incubator) versus the absorbed radiation in turbid coastal waters and applies that correction to the "white" light measured α.

3. Results

3.1. Characteristics of the Hudson river plume

The dynamics of the Hudson River outflow was affected by local winds, bottom topography, and tides. Detailed descriptions of those dynamics are described elsewhere (Choi and Wilkin, 2007; Chant et al., 2008). The majority of the water was entrained within a re-circulating parcel of entrapped low salinity water before it left the New York Bight in a series of coastal jets along New Jersey, Long Island, or the Hudson shelf valley (SV) (Chant et al., 2008, Castelao et al., 2008). As described in Chant et al. (2008), the Hudson's river outflow forms a re-circulating parcel of low salinity water, which was referred to as the "bulge" (Chant et al., 2008), that limited the volume of fresh water advected away in a coastal current. The feature resulted from wind-driven circulation combined by topographic steering (Chant et al., 2008). These "bulges" can extend 30 km from the coast and 40 km in the alongshore direction (panel B in Fig. 1). The water exiting the estuary was characterized by high concentrations of nutrients, non-algal
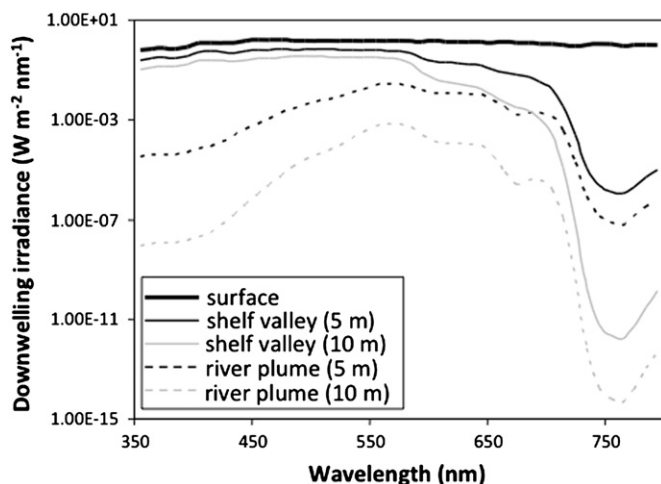

Fig. 2. The spectral irradiance at the surface and two selected depths (5 and 10 m) for two stations occupied during LATTE 2005. The solid lines are the spectral irradiances at the Hudson Shelf Valley, which has a standard offshore marine signature for the Mid-Atlantic Bight (MAB). The dotted lines represent the spectral irradiance within new river (NR) water of the Hudson River. Note the rapid attenuation of blue and red light within the NR waters.
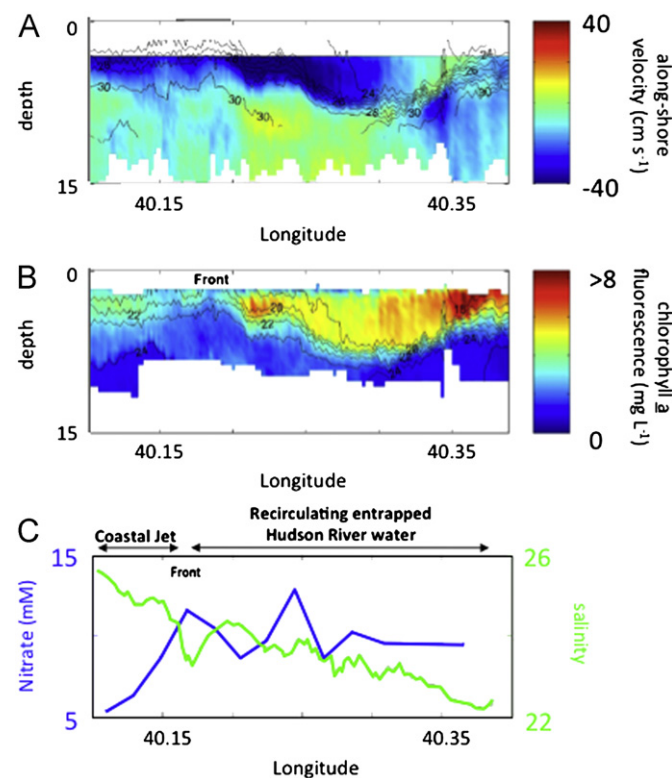

Fig. 3. A transect through the Hudson re-circulating bulge and subsequent coastal jet. (A) The salinity (lines) and the along-shore velocity (color). (B) Density (lines) and chlorophyll a (color). C) The surface salinity (black) and nitrate (red) for the transect.

particles and moderate chlorophyll concentrations (see below), which altered the spectral intensity/quality of the *in situ* light field relative to the offshore coastal waters (Fig. 2). Based on CODAR, moorings, and drifter data the residence time of water in the bulge was calculated to be approximately 4–5 days (Chant et al., 2007). The net result was a buoyant and highly turbid parcel of entrapped low salinity water near the New Jersey coast (Fig. 3).

For this analysis we define 4 water masses based on their salinity and location. Water at the mouth and within Hudson River estuary was defined as New River (NR) water, and was characterized by salinities ≤ 22. As the NR leaves the estuary it is mixed with older water that has been trapped in a re-circulating parcel of low salinity river water which is referred to as "aged river" (AR) water characterized by salinities ranging from 22 to 26 salinity units. The marine waters located offshore and associated with the Hudson Shelf valley are referred to shelf valley waters (SV), and has salinity typical for MAB (≥ 28). Finally, the low salinity AR water eventually leaves the entrapped parcel of re-circulating water near the mouth of the Hudson River estuary and flows southward in a coastal jet. There is water in between the shore and the coastal jet, and we refer to these waters as inshore (IN). These waters have salinities > 26.

The re-circulating bulge of the buoyant Hudson River plume was supplied with NR waters on each tidal cycle, which was rapidly dispersed throughout the entrapped low salinity water near the coast (Chant et al., 2008). The age of the water in the bulge and coastal current was reflected in the nitrate concentration which decreased by over 7-fold as the waters remained in the bulge despite the regular tidal inputs of high nitrate NR waters (Fig. 3C). For example, nitrate concentrations near Sandy Hook in the outflow were 15–20 μM L^{-1} both on April 9 shortly after the beginning of the bulge formation and 6 days later on April 15, indicating a constant input of nutrients into the bulge from the NR waters; however, within the bulge nitrate concentrations decreased from 10–15 μM L^{-1} to 5–10 μM L^{-1} over the 6 day period. During this time the salinity in the bulge remained relatively constant. Note that ammonia concentrations varied from 1 μM in NR plume water to 0.3 μM in AR water. Nitrate concentrations were > 5 μM L^{-1} initially in the coastal current on April 10. By April 13–15 the nitrate concentrations were nearly zero along

the coast. The net result was that little inorganic nitrogen was exported out of these local waters to the wider shelf because of the rapid drawdown of nutrients in the re-circulating parcel of water. Surface nitrate levels in the saline offshore waters (salinities > 28) were under 2 μM. In the bulge, the chlorophyll–nitrate relationship was variable reflecting the mix of the NR and AR. The coastal current was characterized by low nutrients suggesting it was fed by the AR (Fig. 3).

As the nutrients declined within the bulge, phytoplankton biomass increased, which was then subsequently transported in coastal currents along New Jersey or Long island depending on the prevailing wind. One ship survey, within a coastal current typified the high chlorophyll and the depleted nutrients associated with the AR of the bulge (Fig. 3). Based on the frontal propagation speed of the coastal current (Chant et al., 2008), this plume exited the estuary the previous ebb tide. At the edge of the frontal feature surface currents maintained their southern flow, however the plume was thinner, biomass was lower and nitrate levels were declining with time. While some of the reduction in nitrate across the front was due to dilution with ambient shelf waters, surface salinity across the frontal feature only increased by 1–2 salinity units, which would result in only a 20% reduction of nitrate given the lower nitrate concentrations in the SV water. Therefore the reduction of nitrate in the AR was most likely due to assimilation by phytoplankton with estimated nitrogen uptake rates close to 5 μM/day.

Direct measurements of chlorophyll *a* in the river outflow and in the bulge ranged from 17 to 60 mg chl *a* m^{-3}. The HPLC pigments and microscopic analysis indicated the community was dominated by large (> 20 μm) chain forming diatoms. Chlorophyll *a* concentrations inside the AR were high with values as high as 30 mg chl *a* m^{-3}. In contrast, the saline bottom waters below the river plume had lower pigment concentrations with values averaging 8.9 ± 4.8 mg chl *a* m^{-3} and the offshore SV waters had concentrations that averaged 1.5 ± 1.1 mg chl *a* m^{-3}. Associated with high chlorophyll values were extremely high rates of carbon fixation (Fig. 4). Whole community carbon fixation rates in the NR waters were on average 10.8 ± 3.2 mg C m^{-3} h^{-1}. The greater than 20 μm fraction accounted for 81% of the total productivity with 12% and 7% were associated with the 2–20 μm and the < 2 μm
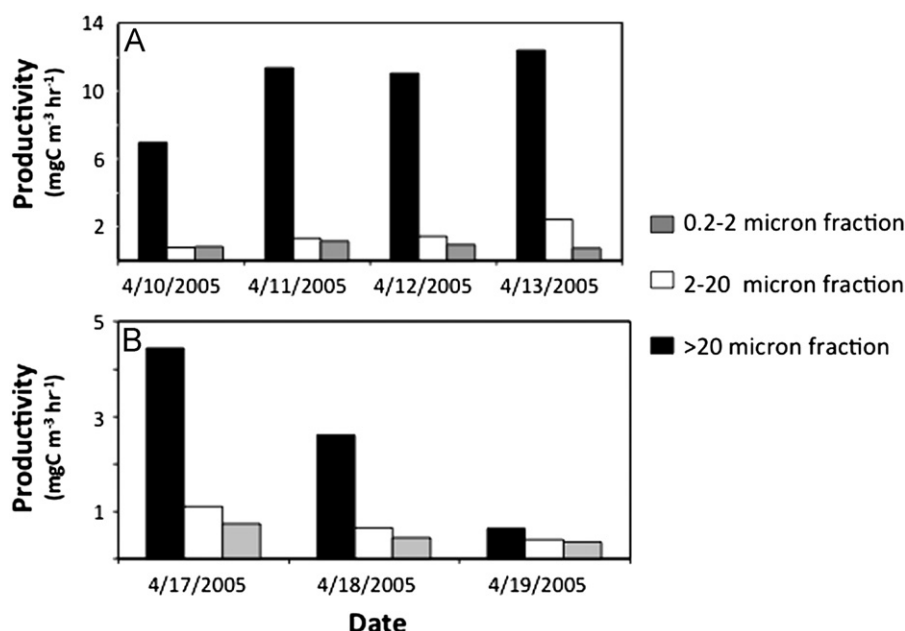

Fig. 4. Surface carbon fixation rates (mg C m^{-3} h^{-1}) within the buoyant plume over time. (A) The phytoplankton productivity size fraction during the formation of the bulge in new river water. (B) The phytoplankton productivity in aged river water.

fractions, respectively. The phytoplankton were healthy with ϕ_{max} values of 0.11 mol C fixed mol^{-1} photons absorbed which is close to the theoretical maximum of 0.125 mol C fixed mol^{-1} photons absorbed (Prézelin et al., 1991). In contrast, the productivity of the AR stations were 3-fold lower with mean community productivity rates of 3.8 ± 2.3 mg C m^{-3} h^{-1}. In the AR rivers the size fractionated productivity was also distinctly different with 67%, 20%, and 14% of the community productivity associated with the $> 20 \mu m$, $2–20 \mu m$, and $< 2 \mu m$ fraction, respectively. In the low nitrate, aged river waters, phytoplankton exhibited signs of stress with ϕ_{max} values dropping by over 5-fold to 0.02 mol C fixed mol^{-1} photons absorbed. Thus the efficiency that absorbed photons were converted into organic carbon varied dramatically within re-circulating bulge based on the availability of nutrients.

High concentrations of phytoplankton, CDOM and non-algal particulates resulted in a turbid plume, however there was significant variability between the colored components that determined the optical properties within the plume (Fig. 5). In the NR waters, CDOM absorption values (Fig. 5A) were 30% higher than phytoplankton and non-algal particulates as waters entered the plume. The phytoplankton and non-algal particle absorption were of similar magnitudes in the NR surface layer. The phytoplankton absorption ratio of 440 to 676 nm was ~0.015 which is consistent with large pigmented phytoplankton cells (Morel and Bricaud, 1981), the size fractionated radio-isotope and microscopic measurements. Total absorption was 3-fold lower in the AR and coastal current plume waters after leaving the bulge. The largest declines in absorption were associated with declines CDOM; however the phytoplankton, and non-algal particulates also exhibited declines (Fig. 5B). Whether the declines in CDOM were due to dilution and/or flocculation, associated with the declines in salinity, with subsequent sinking could not be determined with the available data. The absorption in bottom waters below the AR plume were higher than the surface waters (Fig. 5B), suggesting possible material sinking out of the surface plume to the bottom waters. This hypothesis was consistent with the shipboard visual observations of algal flocs in the surface waters, which potentially

were sinking out of AR surface waters as the phytoplankton became nutrient stressed as indicated by the declines in ϕ_{max}. The AR plume waters had similar absorption magnitudes as non-plume inshore waters (Fig. 5C) characterized by almost no absorption associated with CDOM. This was consistent with the observed declines in oxygen below the AR waters (Fig. 6). The SV waters had very low absorption compared to all other waters (Fig. 5D).

The net result was that the plume was extremely turbid and the incident light field was rapidly attenuated and spectrally skewed (Fig. 2). As the turbidity varied between the major water masses, so did the depth of the 1% light level (Fig. 7). For the NR water the 1% light level was at a 3.4 m depth. In contrast, in the AR waters the 1% light level was 3-fold deeper found at 10.2 m, due to the declines in absorption and decreased scattering. While IN and AR had similar absorption properties (Fig. 7) the 1% light level for IN water was 17.8 m, which was 1.7X deeper than the AR waters. This difference was due to enhanced scattering found within the AR which was on average 30% higher than the IN reflecting the
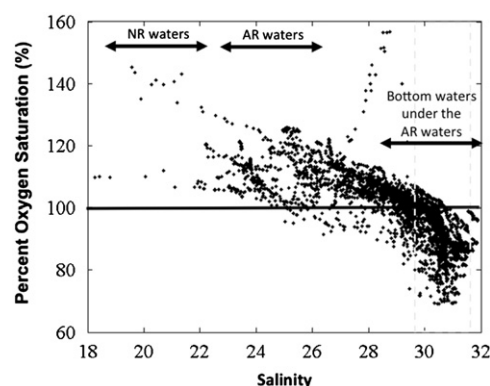

Fig. 6. The oxygen saturation for the surface NR and AR water masses. The saline waters (> 28) are the bottom water beneath the AR outside the mouth of the Hudson River Estuary. The oxygen data was collected with a CTD rosette aboard the RV Oceanus.
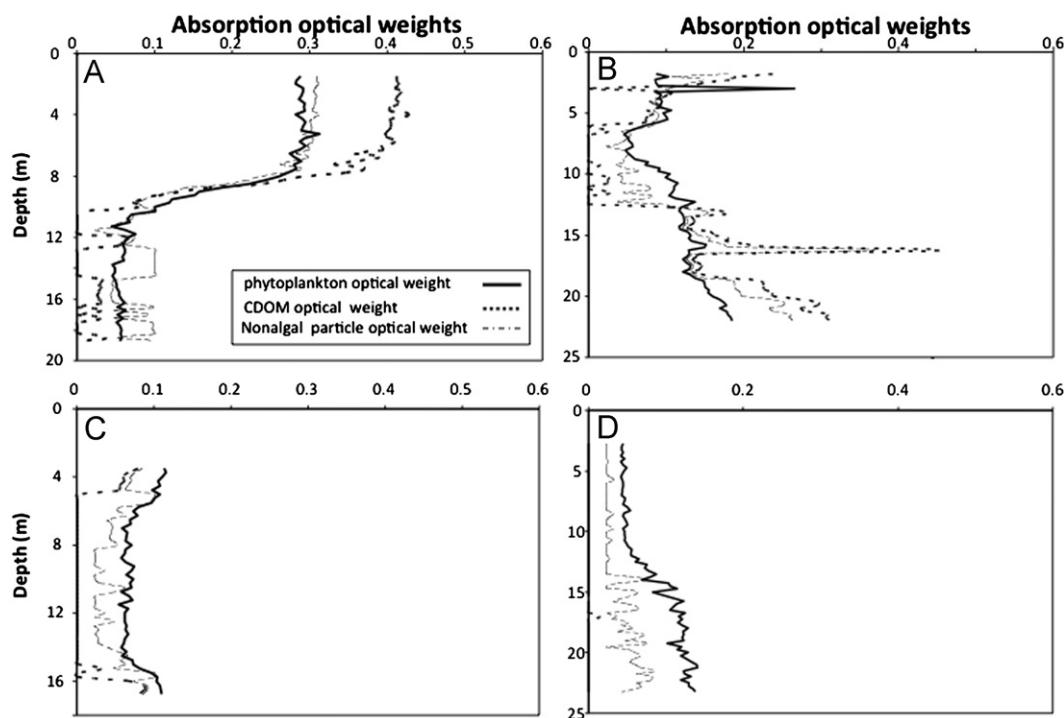

Fig. 5. The optical weights for phytoplankton, CDOM, and nonalgal particles derived from in situ absorption data. The depth profiles for (A) new river (NR), (B) aged river (AR), (C) inshore waters (IN), and (D) shelf valley waters (SV).
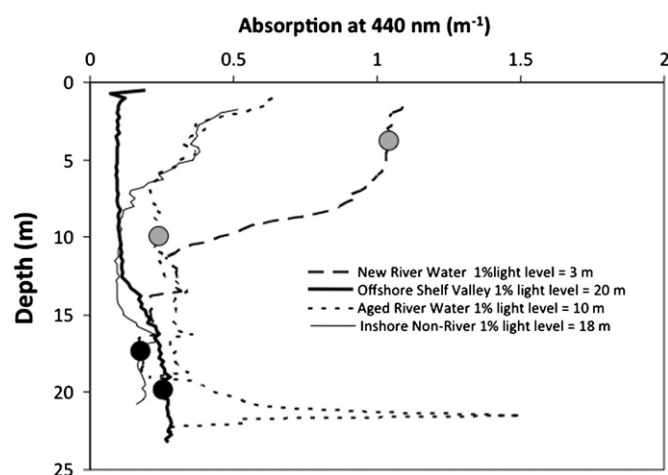
Fig. 7. Profiles of the absorption at 440 nm for new river, aged river, inshore, and shelf valley waters. The black circles indicate the 1% light level for non-river water. The grey circles indicate the 1% light level for river water.
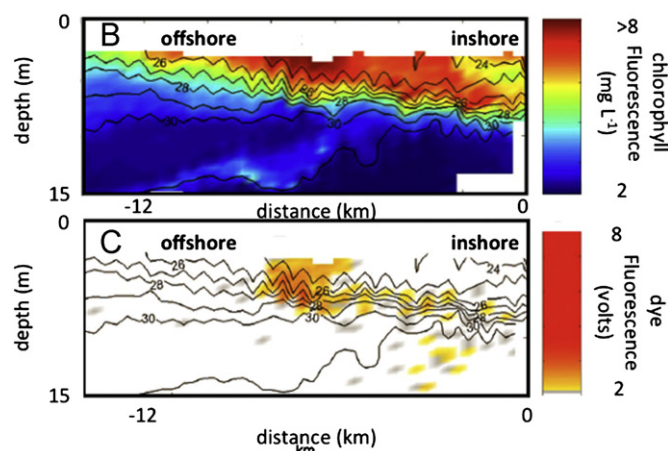

Fig. 8. (A) The chlorophyll a (color) and salinity (lines) during a cross-shelf transect. (C) Rhodamine dye injection in the plume during a cross-shelf transect.

enhanced non-algal particle loads. In contrast the 1% light level for the SV was much deeper at 20.7 m.

3.2. Stratification in the plume

While classic models of river plumes typically characterize the water column in terms of two layers (Yankovsky and Chapman, 1997), water within the plume is usually stratified. Stratification within a plume limits mixing and vertically confines the phytoplankton communities to near surface layers. The rapid attenuation of light and vertical confinement of biomass exerts strong controls over primary production in the nutrient-replete, stratified surface waters. In the plume encountered during LATTE, the confinement of biomass to surface layers enhanced the rapid drawdown of nutrients in the re-circulating bulge above the halocline at 5–8 m below the surface (Fig. 8A and B). The trapping of fluid in the upper layer was confirmed by a dye release (Chant et al., 2008; Houghton et al., 2009), which remained in the upper layer and was confined near a frontal boundary (Fig. 8B). The dye patch was disrupted by an increase in northerly winds, associated with a night-time land breeze (Hunter et al., 2007) that mixed the dye, and phytoplankton, about 55 km offshore. The dispersion of the dye within the plume suggested vertical mixing rates on a time scale of less than a day. The mixing rate potentially allowed phytoplankton to photosynthesize and grow, despite the low light levels within the plume. In the aged plume and coastal jets, the light levels and mixing were higher, but production appeared to be limited by nutrients as suggested by the low *in situ* nutrient concentrations and quantum yields.

Phytoplankton will photoacclimate to maximize the light absorption and photosynthesis whenever possible (Prézelin et al., 1991; Falkowski and Raven, 2007). This is accomplished by the many cellular processes that "tune" E_k to match the *in situ* irradiance (Dubinsky and Schofield, 2009). This results in a depth dependence of P–E parameters. These adjustments can take hours to days depending on the species (Prézelin et al., 1991). If mixing is more rapid than the cell's ability to acclimate, then cells acclimate to the average irradiance and consequently the photosynthetic parameters show little depth dependence (Cullen and Lewis, 1988). Within the NR and AR plume waters, the photosynthetic
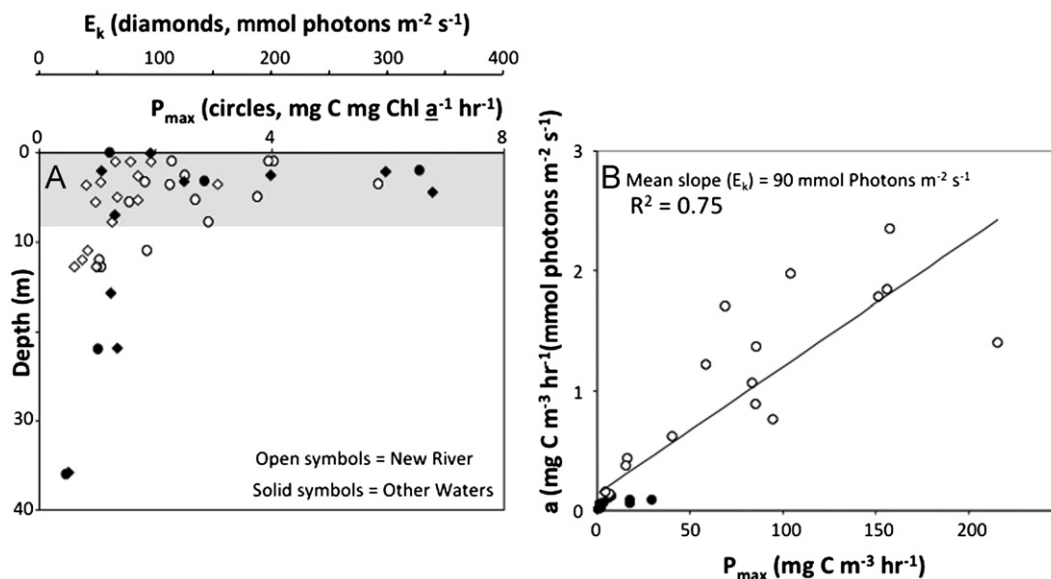

Fig. 9. Photosynthetic characterisitics measured during LATTE 2005. (A) The depth dependent variability in P_{max} chl a^{-1} (circles) and E_k (diamonds). The solid symbols indicate non river waters. The open symbols indicate data collected within the river plume. The grey area indicates the approximate depth of the river waters. (B) The correlation between P_{max} and α. The black symbols indicate non-river waters. The open symbols indicate river water. The slope of the linear line is the average E_k in these waters.

parameters (E_k and P_{max} chl a^{-1}) showed no clear depth dependence suggesting that within the plume mixing exceeded photo-acclimation rates (Fig. 9B). The mean Ek for AR and NR waters was 90 μmol photons $m^{-2} s^{-1}$ (Fig. 9B) as determined by the significant linear correlation between α and P_{max}. Thus mixing confined phytoplankton in the upper plume waters with mixing being more rapid than phytoplankton's ability to photoacclimate. In contrast The E_k values in the offshore SV waters showed a 3-fold decline (to 27 μmol photons $m^{-2} s^{-1}$) with depth indicating photo-acclimation in the offshore waters (Fig. 9). None of the photosynthesis-irradiance curves exhibited photoinihibition during the 2005 experiment.

How important is mixing in the plume to determining the overall primary productivity? We assessed the interaction between mixing, the light field, and the phytoplankton
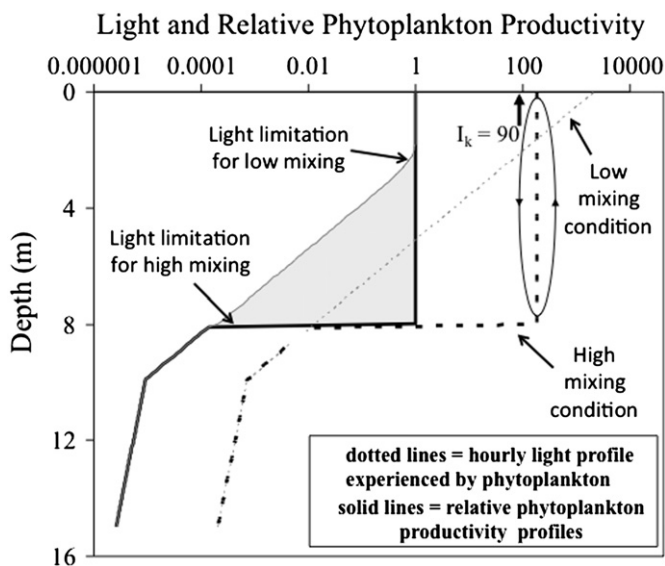

Fig. 10. General schematic of the relationship between mixing and photosynthesis. The figure illustrates the impact of high and low mixing conditions. The dotted lines illustrate the light intensities for high (bold dotted line) and low (fine dotted line) mixing conditions. The respective response of phytoplankton photosynthesis for high (bold) and low (fine) mixing conditions are denoted by solid lines. The photosynthetic response is based on a mean photosynthesis-irradiance curve measured for Hudson plume waters during the 2005 field experiment. The grey shaded area indicates the difference in water column photosynthesis for the high and low mixing conditions.
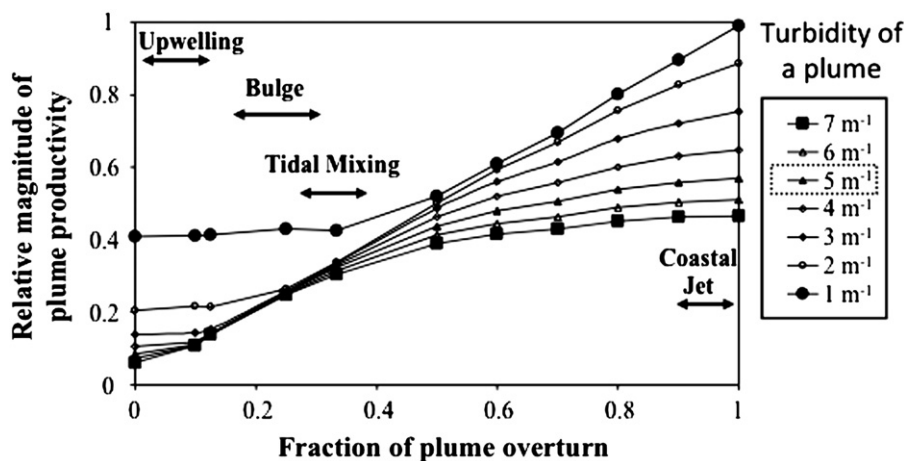
productivity rates within the Hudson river water by determining how the average light experienced by the phytoplankton within the plume impacted the vertically integrated carbon fixation over a range of mixing rates. The productivity rates were calculated by combining the light profiles in the plume with the measured P–E parameters. The variable mixing rates within the plume determined what proportion of the plume phytoplankton are exposed to light levels sufficient to saturate photosynthesis ($E_k < E_d$). An example of this is illustrated in Fig. 10, which shows the light (dotted lines) and the relative phytoplankton productivity rates (solid lines, productivity at depth z divided by P_{max}) for a buoyant plume with no mixing versus that of a full plume overturn in an hour. For the water column with no mixing in an 8 m deep turbid plume, the exponential decrease in light results in phytoplankton being light limited by ~2 m water depth. In a plume, which experiences a full overturn in 1 h, the mean light intensity within the plume is sufficient to saturate photosynthesis throughout the plume. The gray shaded area in Fig. 9, represents the difference in the phytoplankton productivity in a plume with no mixing, 64% lower, compared to a plume that experiences hourly overturn. Thus the mixing within the plume influences the overall productivity of the plume.

Using the mean photosynthesis characteristics measured for the river plume we estimated the relative integrated carbon fixation for a river plume over a range of mixing and turbidity values (Fig. 11). Productivities were scaled relative to the highest productivity, which was observed for rapidly mixing low turbidity waters as no photoinihibition was apparent in the P–E curves. For a range of river turbidities, the integrated photosynthesis declined dramatically as mixing rates decreased. The declines ranged from 30 to 60% depending on the overall turbidity of the river water. Water column productivities also declined by up to 60% as the turbidity of the plume water increased.

4. Discussion

It is critical to understand the transport and the chemical/biological transformation processes within buoyant river plumes, as these processes determine how anthropogenic pollutants enter coastal systems. This has direct implications for water quality management. In a vertically thin plume, light levels can penetrate the plume and this can increase photosynthetic rates and structure the phytoplankton community such as selecting for large (> 50 μm) bloom forming taxa, which in turn will influence food

Fig. 11. The impact of plume mixing on the phytoplankton productivity over a range of turbidities. The turbidity is defined by the attenuation values and the Hudson river plume during the 2005 Latte experiment had attenuation values around 5 m^{-1}. The fraction of plume of overturn defines how rapidly the river water is mixed, with a value of 1 being a full plume overturn in 1 h. The time scales over which different mixing processes impact river plumes in the Mid-Atlantic Bight are indicated by arrows.

web dynamics (Ryther, 1969; Legendre and Rassoulzadegan, 1995). This can accelerate the rate of chemical constituents directly entering the higher trophic levels, which in turn influences the overall bio-accumulation in the food web (Moline et al., 2008). Therefore in urbanized rivers, the physical regulation of the food web is central to understanding the bio-magnification of metals and organic contaminants within coastal marine ecosystems (Pickhardt et al., 2002; Berglund et al., 2001). Unfortunately, understanding the biogeochemical dynamics within coastal buoyant plumes is complex because of the numerous interactions between physics, chemistry, and biology.

The major physical factor dominating the biogeochemistry of the Hudson river plume in spring 2005 was the formation of the re-circulating bulge near the coast. The tendency of the Hudson's outflow to result in a bulge was due to several factors (Chant et al., 2008). A primary factor appeared to be the orientation of the outflow relative to the coast line (Avicola and Huq, 2003; Horner-Devine et al., 2006). Unlike the Chesapeake and Delaware, the Hudson's outflow is not along a straight coastline, but rather flows into an Apex and thus lacks an ambient down shelf flow to press the outflow against the coast. Additionally there is no bathymetric channel to steer the Hudson's outflow towards the coast, as is present at the mouth of the Chesapeake Bay (Valle-Levinson et al., 2007). Finally, the Hudson's outflow is highly stratified which favors bulge formation. Together, coastal morphology and the nature of the outflow favor bulge formation, which in turn modifies the phytoplankton dynamics.

Phytoplankton biomass increases rapidly as the Hudson River plume enters the ocean with populations photosynthesizing at near the theoretical maximum within the re-circulating bulge. The associated high turbidity resulted in light-limited phytoplankton; however mixing rates were sufficiently rapid that the phytoplankton did not induce photoacclimation processes to overcome their overall light limitation (Prézelin et al., 1991, Falkowski and Raven, 2007; Dubinsky and Schofield, 2009). Using the draw down of nitrate as an integrated proxy for total phytoplankton productivity, the integrated daily productivity would be approximated to be close to 400 mg C d^{-1}. The nitrate consumption estimated productivity was 40% lower than the static ship board ^{14}C incubations, which reflects the important role of mixing within the plume to determining the overall productivity of the plume (Figs. 9 and 10). High ^{14}C productivities suggests that static incubation light levels were brighter than the light values encountered by phytoplankton in the plume, despite they were incubated at the average light value within the plume. Reconciling the two estimates would require turnover of the plume to be slow enough to account for the mismatch in the productivities from static incubations and nitrate drawdown. This would be on the order of 2 h.

Are the 2-h estimates of plume mixing reasonable? Upwelling wind transports the plume offshore and "spreads" the water out along the surface. These processes in the Mid-Atlantic bight operate close to local inertial periods (~18 h). In the bulge region, mixing is complex and appears to be influenced by tidal forcing and winds (Chant et al., 2008). The mean dilution rate of dye injected into the re-circulating bulge suggested that mixing time varied from a few hours up to one day (Houghton et al., 2009). Variations in mixing time were dependent on wind forcing and plume configuration. The vertical mixing time of the plume is $T_{\mathrm{mix}} = H^2/(10 \times A_v)$ (Fischer et al., 1979; Geyer et al., 2008) where H is the plume thickness and A_v is vertical eddy diffusivity. Houghton et al. (2009) presents estimates of both H and A_v in river plume based on dye releases during LATTE and of a study of the Delaware River Plume (Houghton et al., 2004). Based on these results T_{mix} ranged from about 1 h in a rapidly advecting coastal current, to 3–4 h during active upwelling favorable winds to 0.5–1 day in the bulge region during moderate winds (rms 8 m s^{-1}) and several

days during times of weak winds (< 2 m s^{-1}). However, in the latter case conditions typically do not remain calm long enough for vertical mixing of the plume to take this long and thus we hypothesize that the upper bound for mixing time rarely exceeds one day. Note that the mean predicted mixing rates were on the order of a few hours, which was close to what is required to reconcile integrated nitrate uptake and ^{14}C productivity estimates.

The feedbacks between mixing and light-limited productivity in extremely turbid environments has been studied extensively for industrial applications however rarely quantified within natural populations. Algal bioreactors have extremely high biomass concentrations that are one- to two-orders of magnitude greater than the Hudson River plume despite the fact that these systems are exponentially more turbid. In these systems, mixing rates increase algal yields by circulating cells between the bright light at the surface of the culture vessel to complete darkness within a few centimeters in the culture (Richmond et al., 1994; Grobbelaar et al., 1995; Doucha and Lívanský, 1995; Lívanský and Doucha, 2005; Doucha et al., 2005). The mixing allows cells to maintain high photosynthetic efficiencies and has been effectively exploited to increase the algal yields (Eriksen, 2008). This is often referred to as the "fluctuating light effect" (Phillips and Myers, 1954; Myers, 1994) and we hypothesize that similar processes are critical to natural populations in turbid coastal buoyant plume waters. This means that calculating the productivity within turbid waters is not possible without quantifying the fluctuating light effect for natural populations, which requires mixing rates within the buoyant plumes to be measured.

High mixing rates in the plume, and the corresponding high productivity rates, result in the build-up of biomass, which in turn has important consequences for the chemistry and physics of local system. Dissolved metal concentrations within the bulge showed enhanced concentrations of iron (Fe), copper (Cu) and zinc (Zn), nickel (Ni), cadmium (Cd), lead (Pb), silver (Ag), and mercury (Hg) (Moline et al., 2008). For all the dissolved metals, the concentrations decreased as salinities increased in the water that exited the bulge and mixed with more saline shelf water; however the concentration of some particulate metals, including Ag, Cu, Fe, and Pb exhibited more complex, nonconservative changes within the bulge indicative of the uptake by suspended particles, including phytoplankton (Moline et al., 2008). Thus factors that regulate the overall growth of the phytoplankton, subsequent grazing and/or sedimentation is critical to understand the offshore transport of metals into the coastal waters of the Mid-Atlantic Bight.

Similarly the physics of the MAB coastal ecosystem will be impacted. Phytoplankton concentrations regulate the radiant transmission and heating rates of the mixed layer (Lewis et al., 1990; Morel and Antoine, 1994; Ohlmann et al., 1996, 1998, 2000; Bissett et al., 2001) and the enhanced near-surface stratification positively feedback on the phytoplankton growth if there is sufficient mixing, which in turn increases near surface local heating (Dickey and Falkowski, 2002). This impact is enhanced in turbid waters (Cahill et al., 2008). Cahill et al. (2008) demonstrated that Hudson river's turbid optical properties were sufficient to alter the surface heat budget by increasing the water temperature and this altered the buoyancy driven circulation. This increased the growth of phytoplankton and modified the plume's optics, which then affected the overall heat budget. This effect in the Hudson plume was sufficient to alter near-shore physical structure and circulation, by enhancing stratification within the plume that confined phytoplankton to the upper water column and accelerating the draw down of nutrients. This stratification however ultimately lowered the potential productivity of the plume by increasing the proportion of the phytoplankton that were chronically light-limited.

In conclusion, bottom topography influenced the circulation of the Hudson River, which trapped buoyant water, and the associated organic material, near the estuarine outflow. In this water mass, phytoplankton productivity rates were high despite that the euphotic zone was very shallow due to high mixing rates within the plume itself that minimized light-limitation due to the fluctuating light effect. These results illustrated the critical importance of measuring the mixing properties within buoyant coastal plumes, as it regulates the potential for biogeochemical transformations of the particulate and dissolved organic matter. Not accounting for fluctuating light effects in these turbid plumes will lead to large errors (~40%) for traditional static biological measurements of phytoplankton productivity. Obtaining estimates of mixing in the photosynthetically active layer of turbid river plumes is challenging because it requires turbulence measurements in the upper few meters of the water column. Field efforts to estimate dissipation rates with microstructure profiling in river plume miss the upper two meters of the water column (Klymak et al., 2006), while measurements with towed vehicles are compromised by the ships wake in the upper ocean. While the use of AUV's to provide near-surface estimates of mixing in river plumes is promising (MacDonald et al., 2007) there have been few field efforts to date and their use in the presence of surface gravity waves are likely to be impaired. Improved understanding the delivery of organic matter from the estuaries to the continental shelf will require thus require development and deployment of a new class of observing technologies.

Acknowledgements

References

Adams, D.A., Connor, O.J.S. Weisbert, S.B., 1998. Sediment Quality of the NY/NJ Harbor System. Final Report. An Investigation Under the Regional Environmental Monitoring and Assessment Program (REMAP) Adams, D. A., O'Connor J. S., Weisberg W. B. U.S. EPA Report EPA/902/R-98/001.

Avicola, G., Huq, P., 2003. The role of outflow geometry in the formation of the re-circulating bulge region in coastal buoyant outflows. Journal of Marine Research 61 (4), 411–434.

Arrigo, K.R., Sullivan, C.W., 1992. The influence of salinity and temperature covariation on the photophysiological characteristics of Antarctic sea ice microalgae. Journal of Phycology 28, 746–756.

Barrick, D.E., 1972. First-order theory and analysis of mf/hf/vhf scatter from the sea. IEEE Transactions on Antennas and Propagation AP-20, 2–10.

Barrick, D.E., Evens, M.W., Weber, B.L., 1977. Ocean surface currents mapped by radar. Science 198, 138–144.

Berglund, O., Larsson, P., Ewald, G., Okla, L., 2001. The effect of lake trophy on lipid content and PCB concentrations in planktonic food webs. Ecology 82, 1078–1088.

Bidigare, R.R., Schofield, O., Prezelin, B.B., 1989. Influence of zeaxanthin on quantum yield of photosynthesis of Synechococcus WH7803 (DC2). Marine Ecology Progress Series 56, 177–188.

Bissett, W.P., Schofield, O., Glenn, S., Cullen, J.J., Miller, W., Pluddeman, A., Mobley, C., 2001. Resolving the impacts and feedbacks of ocean optics on upper ocean ecology. Oceanography 14, 3–53.

Bricaud, A., Morel, A., Prieur, L., 1981. Absorption by dissolved organic matter of the sea (yellow substance) in the UV and visible domains. Limnology and Oceanography 26, 45–53.

Cahill, B., Schofield, O., Chant, R., Wilkin, J., Hunter, E., Glenn, S., Bissett, W.P., 2008. Dynamics of turbid buoyant plumes and the feedbacks on near-shore biogeochemistry and physics. Geophysical Research Letters , http://dx.doi.org/10.1029/2008GL033595.

Castelao, R., Schofield, O., Glenn, S.M., Kohut, J., Chant, R., 2008. Cross-shelf transport of fresh water in the New Jersey Shelf during spring and summer 2006. Journal of Geophysical Research , http://dx.doi.org/10.1029/2007JC004241.

Chant, R.J., Geyer, W.R., Houghton, R., Hunter, E., Lerczak, J., 2007. Estuarine boundary layer mixing processes: insights from dye experiments. Journal of Physical Oceanography 37, 1859–1877.

Chant, R.J., Glenn, S.M., Hunter, E., Kohut, J., Chen, R.F., Houghton, R.H., Bosch, J., Schofield, O., 2008. Bulge formation of a buoyant river outflow. Journal of Geophysical Research 113, C01017, http://dx.doi.org/10.1029/2007JC004100.

Chapman, D.C., Lentz, S.J., 1994. Trapping of a coastal density front by the bottom boundary layer. Journal of Physical Oceanography 24, 1464–1479.

Choi, B.J., Wilkin, J.L., 2007. The effect of wind on the dispersal of the Hudson River plume. Journal of Physical Oceanography 37 (7), 1878–1897.

Cleveland, J.S., Perry, M.J., Kiefer, D.A., Talbot, M.C., 1989. Maximal quantum yield of photosynthesis in the northwestern Sargasso Sea. Journal of Marine Research 47, 869–886.

Crombie, D.D., 1955. Doppler spectrum of sea echo at 13.56 Mc/s. Nature 175, 681–682.

Cullen, J.J., Lewis, M.R., 1988. The kinetics of algal photoadaption in context of vertical mixing. Journal of Plankton Research 10, 1039–1063.

Dickey, T.D., Falkowski, P.G., 2002. Solar energy and its biological-physical interactions in the sea. In: Robinson, A.R., McCarthy, J.J., Rothschild, B.J. (Eds.), The Sea, 12. John Wiley & Sons, pp. 401–440, Chapter 10.

Doucha, J., Lívanský, K., 1995. Novel outdoor thin-layer high density microalgal culture system: productivity and operational parameters. Algological Studies 76, 129–147.

Doucha, J., Straka, F., Lívanský, K., 2005. Utilization of flue gas for cultivation microalgae (Chlorella sp.) in an outdoor open thin-layer photobioreactor. Journal of Applied Phycology 17, 403–412.

Dubinsky, Z., Schofield, O., 2009. Photosynthesis under extreme low and high light in the world's oceans. Hydrobiologia , http://dx.doi.org/10.1007/s10750-009-0026-0.

Eriksen, N.T., 2008. The technology of microalgal culturing. Biotechnology Letters 30, 1525–1536, http://dx.doi.org/10.1007/s10529-008-9740-3.

Falkowski, P.G., Raven, J.A., 2007. Aquatic Photosynthesis. Blackwell Scientific Publishers, Oxford375.

Fan, C.-W. 2002. Bioaccumulation and Air-Water Exchange of the PAH Phenanthrene in Phytoplankton and Raritan Bay, New Jersey. Rutgers University, Ph.D. Diss.

Fischer, H.B., List, E.J., Kho, R.C.Y., Imberger, J., Brooks, N.H., 1979. Mixing in Inland and Coastal Waters. Academic Press, New York 483.

Fong, D.A., Geyer, W.R., 2001. Response of a river plume during an upwelling favorable wind event. Journal of Geophysical Research 106, 1067–1084.

Garvine, R., 1999. Penetration of buoyant coastal discharge onto the continental shelf: a numerical model experiment. Journal of Physical Oceanography 29 (8), 1892–1909.

Geyer, W.R., Chant, R., Houghton, R., 2008. Tidal and spring-neap variations in horizontal dispersion in a partially mixed estuary. Journal of Geophysical Research 113, C07023, http://dx.doi.org/10.1029/2007JC004644.

Glenn, S.M., Arnone, R., Bergmann, T., Bissett, W.P., Crowley, M., Cullen, J., Gryzmski, J., Haidvogel., D., Kohut, J., Moline, M.A., Oliver, M., Orrico, C., Sherrell, R., Song, T., Weidemann, A., Chant, R., Schofield, O., 2004. The biogeochemical impact of summertime coastal upwelling in the Mid-Atlantic Bight. Journal of Geophysical Research 109, C12S02, http://dx.doi.org/10.1029/2003JC002265.

Glenn, S.M., Schofield, O., 2003. Observing the oceans from the COOL room: our history, experience, and opinions. Oceanography, 16; 37–52.

Green, S.A., Blough, N.V., 1994. Optical absorption and fluorescence properties of chromophoric dissolved organic matter in natural waters. Limnology and Oceanography 39, 1903–1916.

Grobbelaar, J.U., Nedbal, L., Tichý, V., Šetlík, I., 1995. Variation in some photosynthetic characteristics of microalgae cultured in outdoor thin-layered sloping reactors. Journal of Applied Phycology 7, 84–175.

Horner-Devine, A.R., Fong, D.A., Monismith, S.G., Maxworthy, T., 2006. Laboratory experiments simulating a coastal river outflow. Journal of Fluid Mechanics, 203–232.

Houghton, R.W., Chant, R.J., Rice, A., Tilburg, C., 2009. Salt flux into coastal river plumes: dye studies in the Delaware and Hudson River outflow. Journal of Marine Research 67, 731–756.

Houghton, R.W., Tilburg, C.E., Garvine, R.W., Fong, A., 2004. Delaware River plume response to a strong upwelling-favorable wind event. Geophysical Research Letters 31, L07302, http://dx.doi.org/10.1029/2003GL018988.

Howarth, R.W., Marino, R., Swaney, D.P., Boyer, E.W., 2006. Wastewater and watershed influences on the primary productivity and oxygen dynamics in the lower Hudson River estuary. In: Levington, J.S., Waldman, J.R. (Eds.), The Hudson River Estuary. Cambridge University Press, New York, pp. 121–139.

Hunter, E., Chant, R., Bowers, L., Glenn, S., Kohut, J., 2007. Spatial and temporal variability of diurnal wind forcing in the coastal ocean. Geophysical Research Letters 34, L03607, http://dx.doi.org/10.1029/2006GL028945.

Jeffrey, S.W., Mantoura, R.F.C., Wright, S.W., 1997. Phytoplankton pigments in oceanography. United Nations Educational, Scientific and Cultural Organization, Paris 661.

Johnson, D.R., Schofield, O., Miller, J., 2003. Dynamics and optics of the Hudson River outflow. Journal of Geophysical Research 108 (C10), 3323, http://dx.doi.org/10.1029/ 2002JC001485.

Johnsen, G., Samset, O., Granskog, L., Sakshaug, E., 1994. In vivo absorption characteristics in 10 classes of bloom-forming phytoplankton: Taxonomic characteristics and responses to photoadaptation by means to discriminant and HPLC analysis. Marine Ecology Progress Series 105, 149–157.

Kalle, K., 1966. The problem of the Gelbstoff in the sea. Marine Biology Review 4, 91–104.

Kohut, J.T., Glenn, S.M., 2003. Improving HF radar surface current measurements with measured antenna beam patterns. Journal of Atmospheric and Oceanic Technology 20, 1303–1316.

Kohut, J.T., Glenn, S.M., Chant, R.J., 2004. Seasonal current variability on the New Jersey inner shelf. Journal of Geophysical Research 109 (C07S07), http://dx.doi.org/10.1029/2003JC001963.

Klymak, J.M., Moum, J.N., Nash, J.D., Kunze, E., Girton, J.B., Carter, G.S., Gregg, M.C., 2006. An estimate of tidal energy lost to turbulence at the Hawaiian Ridge. Journal of Physical Oceanography 36 (6), 1148–1164.

Latasa, M., Bidigare, R.R., Ondrusek, M.E., Kennicutt, M.C., 1996. HPLC analysis of algal pigments: a comparison exercise among laboratories and recommendations for improved analytical performance. Marine Chemistry 51, 315–324.

Legendre, L., Rassoulzadegan, F., 1995. Plankton and nutrient dynamics in marine waters. Ophelia 41, 153–172.

Lewis, M.R., Carr, M.-E., Feldman, G.C., Esaias, W., McClain, C., 1990. Influence of penetrating solar radiation on the heat budget of the equatorial Pacific Ocean. Nature 347, 543–545.

Lívanský, K., Doucha, J., 2005. Utilization of carbon dioxide by *Chlorella kessleri* in outdoor open thin-layer culture units. Archives of Hydrobiology 157, 201–212.

MacDonald, D.G., Goodman, L., Hetland, R.D., 2007. Turbulent dissipation in a near-field river plume: a comparison of control volume and microstructure observations with a numerical model. Journal of Geophysical Research 112, C07026.

Malone, T., Chervin, B., 1979. The production and fate of phytoplankton size fractions of the Hudson River, New York Bight. Limnology and Oceanography 24, 683–696.

Malone, T., Conley, D.J., Fisher, T.R., Glibert, P.M., Harding, L.W., Sellner, K., 1996. Scales of nutrient limited phytoplankton productivity in Chesapeake Bay. Estuarine 19 (2B), 33–85.

Mobley, C.D., 1994. Light and Water Radiative Transfer in Natural Waters. Academic Press, San Diego 591.

Moline, M.A., Frazer, T.K., Chant, R., Glenn, S., Jacoby, C.A., Reinfelder, J.R., Yost, J., Zhou, M., Schofield, O., 2008. Biological responses in a dynamic, buoyant river plume. Oceanography 21 (4), 91–107.

Morel, A., Antoine, D., 1994. Heating rate within the upper ocean in relation to its bio-optical state. Journal of Physical Oceanography 24, 1652–1665.

Morel, A., Bricaud, A., 1981. Theoretical results concerning light absorption in a discrete medium, and application to specific absorption of phytoplankton. Deep Sea Research 28, 1375–1393.

Morel, A., Smith, R.C., 1974. Relation between total quanta and total energy for aquatic photosynthesis. Limnology and Oceanography 19 (4), 591–600.

Munchow, A., Garvine, R.W., 1993. Dynamical properties of a buoyancy-driven coastal current. Journal of Geophysical Research 98 (C11), 20063–20078.

Myers, J., 1994. The 1932 experiments. Photosynthesis Research 40, 303–310.

Ohlmann, J.C., Siegel, D.A., Gautier, C., 1996. Ocean mixed layer radiant heating and solar penetration: a global analysis. Journal of Climate 9, 2265–2280.

Ohlmann, J.C., Siegel, D.A., Washburn, L., 1998. Radiant heating of the western equatorial Pacific during TOGA-COARE. Journal of Geophysical Research 103, 5379–5395.

Ohlmann, J.C., Siegel, D.A., Mobley, C.D., 2000. Ocean radiant heating. Part I: Optical influences. Journal of Physical Oceanography 30, 1833–1848.

Oliver, M.J., Schofield, O., Bergmann, T., Glenn, S., Orrico, C., Moline, M., 2004. Deriving *in situ* phytoplankton absorption for bio-optical productivity models in turbid waters. Journal of Geophysical Research 109 (C07S11), http://dx.doi.org/10.1029/2002JC001627.

Pegau, S.W., Cleveland, J., Doss, W., Kennedy, D.C., Maffione, R.A., Mueller, J.L., Stone, R., Trees, C.C., Weidemann, A.D., Wells, W.W., Zaneveld, R.J., 2001. A comparison of methods for the measurement of the absorption coefficient in natural water. Journal of Geophysical Research 100, 13201–13221.

Phillips, J.N., Myers, J., 1954. Growth rate of Chlorella in flashing light. Plant Physiology 29, 152–161.

Pickhardt, P.C., Folt, C., Chen, C., Klaue, B., Blum, J., 2002. Algal blooms reduce the uptake of toxic methyl-mercury in freshwater food webs. Proceedings of the National Academy of Sciences of the United States of America 99, 4419–4423.

Prézelin, B.B., Boucher, N.P., Moline, M., Stephens, E., Seydel, K., Scheppe, K., 1992. PALMER LTER: spatial variability in phytoplankton distribution and surface photosynthetic potential within the Peninsula grid, November 1991. Antarctic Journal of the United States 27, 242–244.

Prézelin, B.B., Tilzer, M.M., Schofield, O., Haese, C., 1991. The control of the production process of phytoplankton by the physical structure of the aquatic environment with special reference to its optical properties. Aquatic Sciences 53, 136–186.

Richmond, A., Boussiba, S., Vonshak, A., Kopel, R., 1994. A new tubular reactor for mass production of microalgae outdoors. Journal of Applied Phycology 5, 32–327.

Ryther, J.H., 1969. Photosynthesis and fish production in the Sea. Science 166, 72–76.

Sanudo-Wilhelmy, S.A., Gill, G.A., 1999. Impact of the Clean Water Act on the levels of toxic metals in urban estuaries: the Hudson River estuary revisited. Environmental Science and Technology 33, 3477–3481.

Schofield, O., Bergmann, T., Bissett, W.P., Grassle, F., Haidvogel, D., Kohut, J., Moline, M.A., Glenn, S., 2002. Linking regional coastal observatories to provide the foundation for a national ocean observation network. Journal of Oceanic Engineering 27, 146–154.

Schofield, O., Bergmann, T., Oliver, M., Irwin, A., Kirkpatrick, G., Bissett, W.P., Orrico, C., Moline, M.A., 2004. Inversion of spectral absorption in the optically complex coastal waters of the Mid-Atlantic Bight. Journal of Geophysical Research 109 (C12S04), http://dx.doi.org/10.1029/2003JC002071.

Schofield, O., Bosch, J., Glenn, S., Kirkpatrick, G., Kerfoot, J., Lohrenz, S., Moline, M.A., Oliver, M., Bissett, W.P., 2007. Bio-optics in integrated ocean observing networks: the potential for studying harmful algal blooms. In: Babin, M., Roesler, C.S., Cullen, J.J. (Eds.), Real-time Observation Systems for Ecosystem Dynamics and Harmful Algal Blooms. UNESCO, Paris.

Schofield, O., Kerfoot, J., Mahoney, K., Moline, M., Oliver, M., Lohrenz, S., Kirkpatrick, G., 2006. Vertical migration of the toxic dinoflagellate Karenia brevis and the impact on ocean optical properties. Journal of Geophysical Research 111, C06009, http://dx.doi.org/10.1029/2005JC003115.

Schofield, O., Kohut, J., Glenn, S., Morell, J., Capella, J., Corredor, J., Orcutt, J., Arrott, M., Krueger, I., Meisinger, M., Peach, C., Vernon, F., Chave, A., Chao, Y., Chien, S., Thompson, D., Brown, W., Oliver, M., Boicourt, W, 2010. A regional Slocum glider network in the Mid-Atlantic coastal waters leverages broad community engagement. Marine Technology Society 44 (6), 1–11.

Schofield, O., Bidigare, R.R., Prézelin, B.B., 1990. Spectral photosynthesis, quantum yield and bluegreen light enhancement of productivity rates in the diatom *Chaetoceros gracile* and the prymnesiophyte *Emiliania huxleyi*. Marine Ecology Progress Series 64, 175–186.

Smith, R.C., Prezelin, B.B., Bidigare, R.R., Baker, K.S., 1989. Bio-optical modeling of photosynthetic production. Limnology and Oceanography 34, 1526–1546.

Stewart, R.H., Joy, J.W., 1974. HF radio measurements of ocean surface currents. Deep Sea Resear 21, 1039–1049.

Tanada, T., 1951. The photosynthetic efficiency of carotenoid pigments in Navicula minima. American Journal of Botany 38, 276–283.

Valle-Levinson, A., Holderied, K., Chant, R.J., 2007. Subtidal flow structure at the turning region of a wide outflow plume. Journal of Geophysical Research 112, C04004, http://dx.doi.org/10.1029/2006JC003746.

Van Heukelem, L., Thomas, C., 2001. Computer-assisted high-performance liquid chromatography method development with applications to the isolation and analysis of phytoplankton pigments. Journal of Chromatography 910, 31–49.

Yankovsky, A., Chapman, D., 1997. A simple theory for the fate of buoyant coastal discharges. Journal of Physical Oceanography 27 (7), 1386–1401.